Interhemispheric influence of surface buoyancy conditions on a circumpolar current

Neven S. Fučkar[1] and Geoffrey K. Vallis[1,2]

Received 14 April 2007; revised 9 June 2007; accepted 25 June 2007; published 24 July 2007.

[1] This study shows that the surface buoyancy conditions in the Northern Hemisphere may influence the stratification and transport of the Antarctic Circumpolar Current (ACC). We use a course-resolution ocean general circulation model (OGCM) in an idealized single-basin configuration with a circumpolar channel. A decrease in the magnitude of the surface temperature meridional gradient in the Northern Hemisphere reduces production of the deep water, affecting the interhemispheric Meridional Overturning Circulation (MOC) and deepening the thermocline in both hemispheres. The induced change of stratification in the Southern Hemisphere circumpolar region increases the zonal volume transport of circumpolar current because of an increase in the local meridional density gradient and the associated thermal wind shear, which is the dominant baroclinic component of the total volume transport. The result is robust to variations in the background vertical mixing and the parameterization scheme for mesoscale eddies. **Citation:** Fučkar, N. S., and G. K. Vallis (2007), Interhemispheric influence of surface buoyancy conditions on a circumpolar current, *Geophys. Res. Lett.*, *34*, L14605, doi:10.1029/2007GL030379.

1. Introduction

[2] A number of studies encompassing the nature of the deep MOC cell, involving the southward North Atlantic Deep Water (NADW) flow and the northward upper ocean flow, have shown a potential for a significant cross-equatorial influence of surface boundary conditions on elements of the combined MOC-ACC system. For example, *Toggweiler and Samuels* [1995, 1998] show that increasing the amplitude of winds south of 30°S increases the NADW production and the pycnocline depth north of the ACC. Consistently, *Gnanadesikan and Hallberg* [2000] shows that both dynamic and thermodynamic balances are important in the equilibrium state of the ACC and the MOC, and *Vallis* [2000] notes the controlling effect that a circumpolar channel has on the interhemispheric structure of the MOC, including its sensitivity to the location where the densest surface water is formed.

[3] Of particular relevance to this study *Samelson* [1999] first presents a simple analytical model of the large-scale dynamics of a circumpolar current that requires surface wind, but is primarily determined by the surface buoyancy forcing around the circumpolar channel in connection with equatorward structure of the thermocline. *Samelson* [2004] expands this picture and suggests the possibility of an influence of the northern hemisphere surface boundary conditions on the southern hemisphere circumpolar current. Motivated in part by this, we explore how the northern hemisphere surface buoyancy change affects the structure of the MOC and the thermocline in both hemispheres, and the consequent effect on the density structure and transport of the southern hemisphere circumpolar current in an idealized numerical setup.

2. Model and Experiments

[4] We employ a simplified configuration of the Modular Ocean Model version 4.0c [*Griffies et al.*, 2004]. Our model has a flat-bottomed single-basin geometry with a horizontal resolution of 2° × 2° and 30 vertical levels of thickness varying from 10 m at the top to 290 m at the bottom. The basin zonal width is 60° and the meridional span is from 72°S to 72°N. The Southern Hemisphere contains a simplified version of the Drake Passage-a zonal channel 4° long, extending from 64°S to 54°S, with a 2555 m deep sill and a basin-periodic eastern boundary.

[5] We conduct two sequences of experiments with different profiles of background vertical mixing. The first sequence has a constant vertical diffusivity coefficient κ_v of 0.15 cm^2s^{-1} matching direct measurements in the main thermocline [e.g., *Ledwell et al.*, 1998]. The other sequence has a Bryan–Lewis type of vertical mixing profile [*Bryan and Lewis*, 1979] that has an order of magnitude higher vertical diffusivity in the abyss (curve *ii* in Figure 1b). A convective scheme for vertical adjustment of unstable water column is implemented following *Rahmstorf* [1993]. We use the Gent-McWilliams skew flux scheme combined with downgradient neutral diffusion to parameterize effects of mesoscale eddies. The used eddy tracer diffusivity is proportional to the vertically averaged horizontal density gradient, ranging from 100 m^2s^{-1} to 1000 m^2s^{-1} in the interior with conversion to horizontal diffusion within the surface boundary layer. We employ a horizontal Laplacian friction with the Smagorinsky viscosity closely based on OM3.1 setup [*Griffies et al.*, 2005] that yields the viscosity coefficient in range from 15500 m^2s^{-1} to 110271 m^2s^{-1}.

[6] The surface heat and fresh water fluxes are treated via restoring conditions on temperature and salinity at the top level. We use a thermal restoring coefficient of approximately 47 $Wm^{-2}K^{-1}$, equivalent to a 10-day restoring timescale (also used for salinity), given our top level thickness of 10 m. Applied annual mean zonally uniform SST and surface salinity are the analytical constructs roughly based on the annual global zonal mean observations from the NODC's World Ocean Atlas 2001 [*Conkright et al.*, 2002, hereinafter referred to as WOA01]. Our focus is on

[1] Atmospheric and Oceanic Sciences Program, Princeton University, Princeton, New Jersey, USA.
[2] NOAA Geophysical Fluid Dynamics Laboratory, Princeton, New Jersey, USA.

0094-8276/07/2007GL030379$05.00

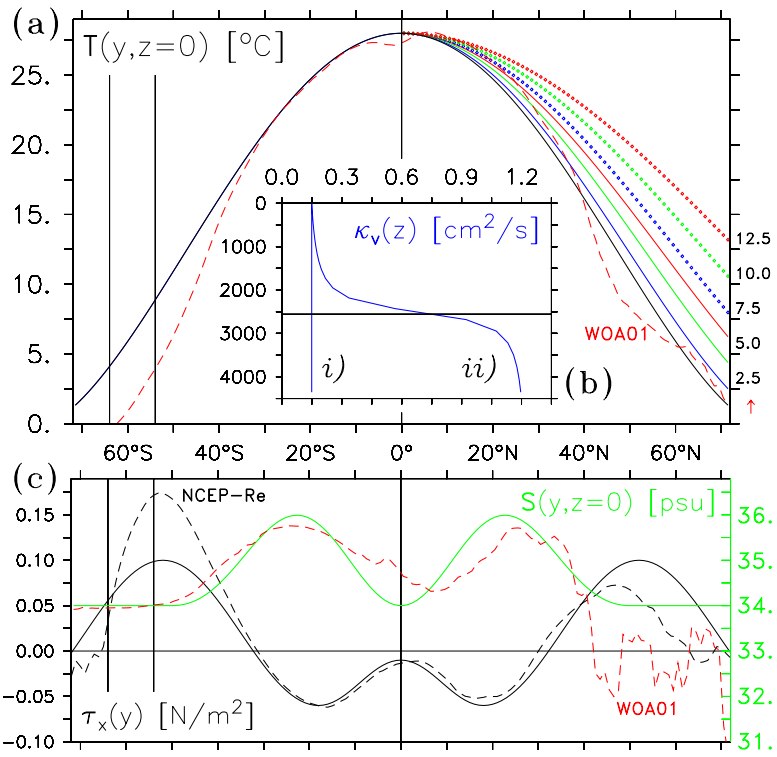

Figure 1. (a) The annual mean longitudinally invariant SST restoring fields. The solid black line represents the hemispherically symmetric control case, while the solid and dotted colored lines show asymmetric perturbations depicting increasing levels of the hypothetical NH warming. The dashed red line shows the annual global zonal mean of the observed SST from WOA01. The vertical lines around 60° S represent the boundaries of the model's Drake Passage. (b) The two applied options of vertical mixing profile: (*i*) a constant value of the vertical diffusivity κ_v of 0.15 cm^2s^{-1}, and (*ii*) a Bryan–Lewis type profile. The horizontal line at the depth of 2555 m marks the sill level of the Drake Passage. (c) The annual zonally uniform surface salinity restoring field (solid green line) and the zonal wind stress (solid black line). The dashed red line shows the annual global zonal mean of the observed surface salinity from WOA01, and the dashed black line shows the global zonal mean of the last 20 years of zonal wind stress from NCEP-Re.

thermal effects, hence we use a hemispherically symmetric distribution of the surface salinity (Figure 1c) and the sequences of increasing northern hemisphere SST restoring fields, as in Figure 1a. The annual surface momentum flux is implemented via zonally uniform zonal wind stress (Figure 1c), roughly based on the global zonal mean of the last 20 years of the NCEP-NCAR reanalysis [*Kalnay et al.*, 1996, hereinafter referred to as NCEP-Re], but again we impose hemispheric symmetry. Thus, purposely the only sources of interhemispheric asymmetry in our experiments are the SST fields and the circumpolar channel.

[7] The sequence of equilibration experiments for both vertical mixing profiles starts with the control case that has all surface forcing fields hemispherically symmetric. Our model reaches a state close to the equilibrium after 2500 years of the integration. From this state we start the set of the surface buoyancy perturbation experiments forced with increasing levels of the northern hemisphere surface temperature shown in Figure 1a. The near-equilibrium states are again achieved after 2500 years.

3. Results

3.1. Change of the MOC and Stratification

[8] For the set of experiments with a Bryan–Lewis type of vertical mixing, Figure 2 shows that increasing the northern hemisphere surface buoyancy (due to SST changes in Figure 1a) reduces the northern hemisphere deep water formation and the deep MOC cell. The decreasing zonally averaged depth of an isotherm of the rising coldest SST in the Northern Hemisphere (blue line in Figure 2) indicate a decrease of the water column part directly fed by the northernmost surface region in the perturbation cases. This allows more substantial formation and input of intermediate water at greater depth just north of the Drake Passage (Figure 2b) and eventually its intrusion into the Northern Hemisphere (Figure 2c).

[9] The thermocline structure and related partition of the ocean between the light and dense waters change. Let us choose the 10°C isotherm as a boundary between the warm, upper, waters and the cold, deep and abyssal, waters, and label its depth z_{10}. This isotherm (red line in Figure 2) is often associated with the Subtropical Front (the northern edge of the Southern Ocean) and it roughly corresponds to the depth of the main thermocline in the subtropical gyres. Reducing the magnitude of the northern hemisphere SST meridional gradient increases z_{10} (Figures 2a, 2b, and 2c) as might be expected from standard thermocline theory scaling [e.g.,*Vallis*, 2006]. *Gnanadesikan* [1999] and *Samelson* [2004] note, in different contexts, the importance of the water mass conversion balance to achieve an equilibrium state, i.e., the conversion rate of light to dense water must

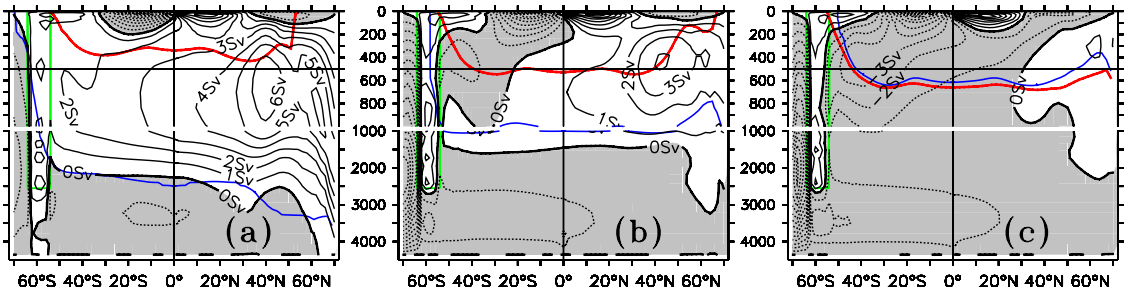

Figure 2. The annual mean state after 2500 years of integration for experiments with three different SST conditions, using a Bryan-Lewis type of vertical mixing. The contours show the residual (Eulerian mean plus eddy-induced contribution) MOC volume transport streamfunction ψ in Sverdrups (1 Sv = 10^6 m^{3}s^{-1}). The negative values are shaded and the top 1 km is expanded. The zonally averaged depth of 10°C isotherm (z_{10}) is overlaid as a red line, while the zonally averaged isotherm of the coldest northernmost surface water is overlaid as a blue line. (a) The symmetrical control case (associated with the black line in Figure 1a). (b) The perturbation case with +4.9°C increase in the coldest northernmost restoring SST (the solid red line in Figure 1a). (c) The case with +9.3°C equivalent increase (the dotted green line in Figure 1a). The model's Drake Passage is outlined in green. (The apparent intersection of ψ contours with the northern and southern boundary where $\psi = 0$ is an artifact of contouring.)

balance the conversion rate of dense to light water. In a perturbation case the northern hemisphere transformation of light to dense water diminishes because the northern hemisphere surface warms, hence the volume of light water expands – an indicator of deepening of the thermocline. The deep MOC cell reverses after the northern hemisphere warming crosses a threshold at which all of the northern hemisphere surface waters are lighter than the surface water just north of the Drake Passage (e.g., Figure 2c).

[10] Another aspect of the induced MOC change is the intensification of the abyssal MOC cell involving the northward flow of the bottom water and the southward return flow at the mid-depth. The reduction of the deep MOC cell in a perturbation case enables the development of a stronger abyssal MOC cell presumably because the background vertical mixing is capped by the weaker advection of warmer and shallower northern hemisphere deep water. The overturning subcell south of the Drake Passage intensifies because its sinking branch supplies the densest surface water to the more vigorous abyss. The meridional flow bellow the Drake Passage sill enforces the intensification of the southernmost subcell (centered south of the gap) relative to the bottom subcell (centered below the sill) roughly by the inverse ratio between their domains as the linear coefficient of proportionality.

3.2. Change of the ACC Volume Transport

[11] A reduction of the northern hemisphere deep water formation (represented by the black line in Figure 3a) and consequent cross-equatorial deepening of the thermocline (roughly captured by the red line in Figure 3a) cause a substantial increase of the zonal volume transport of the model's ACC (e.g., the black line in Figure 3b). A longitude in the Drake Passage is chosen for Figure 3 to avoid variability of the model's ACC meridional extent in zonal direction, but this increase of the circumpolar volume transport persists throughout the model's Southern Ocean. The increase of volume transport occurs primarily in the baroclinic component, or more precisely, its part associated with the meridional density gradient across the southern hemisphere circumpolar region via the thermal wind balance; $f\,\rho_o\partial_z\,u = g\partial_y\rho$ (in the Boussinesq approximation). Elaborating on this, we decompose the volume transport through the Drake Passage into the barotropic and baroclinic components. The barotropic component is defined as a vertical integral, from the Drake Passage sill level up to the surface, of a zonal velocity at the sill level (blue line in Figure 3b). The baroclinic component is a difference between the total transport and the barotropic component. The baroclinic component may be further decomposed into the geostrophic part determined by the thermal wind relation (red line in Figure 3b) and an ageostrophic, primarily frictional, part (green line in Figure 3b), which is the overall baroclinic transport minus the geostrophic part.

[12] The warming of the northern hemisphere surface leads to the weakening and shoaling of the deep western boundary current which is the interhemispheric conveyor of the northern hemisphere deep water into the Southern Ocean. The mass balance of the meridional flow in the model's Southern Ocean is primarily between the northward surface Ekman transport and the net southward geostrophic flow below the sill of the Drake Passage; the latter is intensified in lateral boundary regions and has a peak in the vertical close to the sill level. The mean southward geostrophic flow above the sill level vanishes because there is no means to maintain a net zonal pressure gradient throughout a zonally unbounded region. The eddy-induced or bolus meridional transport is present above and below the sill level of the Drake Passage. The vertically integrated (parameterized) bolus transport vanishes, but it changes the vertical distribution of meridional flow. Specifically, there is a net southward bolus transport above the sill localized close to the northern edge of the Drake Passage compensated by the matching net northward bolus transport below the sill.

[13] The increase of the northern hemisphere surface buoyancy increases the subsurface meridional density gradient in the southern hemisphere circumpolar region due to the deepening of the stratification profile north of the model's Southern Ocean (i.e., an expansion of the light water domain). *Samelson* [1999, 2004] describes how the presence of a finite-depth sill in conjunction with the

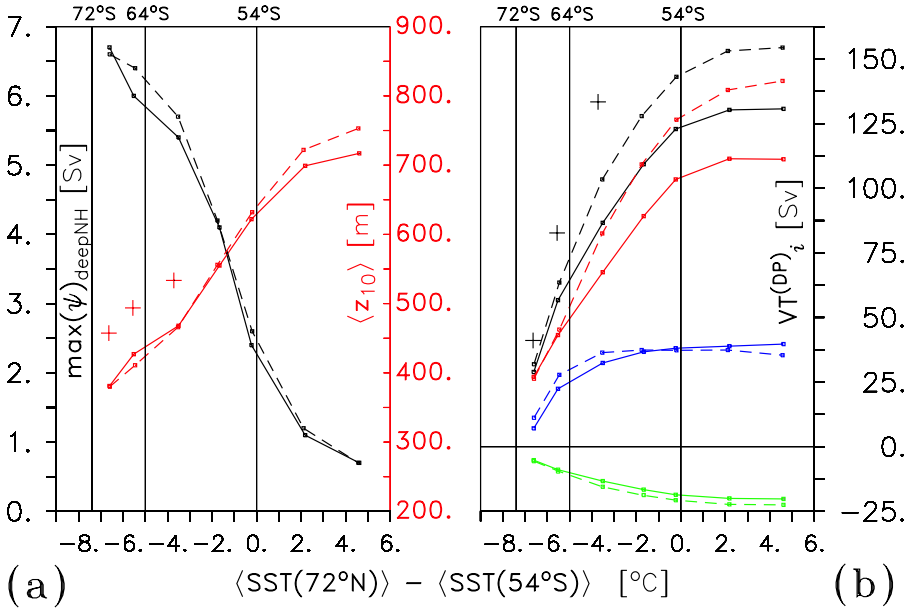

Figure 3. Various quantities as a function of the difference between the zonal average of the northernmost SST and SST at the northern edge of the model's Drake Passage in the final annual mean states (after 2500 years) using a Bryan–Lewis type of vertical mixing (solid lines) and a constant vertical mixing (dashed lines). Crosses represent experiments with a constant vertical mixing and doubled amplitude of the Southern Hemisphere westerlies. Vertical lines and associated latitudes mark the southern edge of the basin and the southern and northern edge of the Drake Passage. (a) Black lines: deep water production (i.e., deep maximum of overturning streamfunction ψ) in the Northern Hemisphere. Red lines and crosses: basin average from 40°S to 40°N of z_{10}. (b) Black lines and crosses: total zonal volume transport through the Drake Passage. Blue lines: barotropic part. The red and green lines are the baroclinic geostrophic and the baroclinic ageostrophic parts, respectively.

meridional surface density gradient across the Drake Passage can establish a thermal circumpolar current in a simple analytical model with adiabatic interior and no eddies. In our model the mechanism is changed by the presence of vertical mixing and parameterized eddies. In particular, the Southern Ocean residual (i.e., the Eulerian mean plus bolus) southward flow effectively advects the influence of the perturbed stratification north of the Drake Passage into the circumpolar region; the vertical diffusion and bolus transport relax the constraint of conveying the northern hemisphere surface thermal perturbation southward though the model's Southern Ocean only beneath the sill level as required in adiabatic non-eddying model. The surface divergence in the Southern Ocean pulls intermediate and deep water toward the surface, most importantly just south of the Drake Passage from below the sill. This upwelling controls the stratification just south of the Drake Passage, which is rather invariant in all experiments. Hence, the deepening of the thermocline just north of the Drake Passage increases the meridional density gradient between the northern and southern edge of the Drake Passage causing an increase in the thermal wind part of circumpolar transport.

[14] The northern hemisphere surface warming causes an increase in the circumpolar volume transport if the northernmost SST matches the SST somewhere in the model's Southern Ocean – the states left from 54°S vertical line in Figure 3. The increasing surface thermal perturbation eventually leads to states with the northernmost SST matching the SST north of the Drake Passage–the states right from 54°S vertical line in Figure 3. Then the Ekman transport at the northern edge of the Drake Passage contains the densest surface water north of the Southern Ocean and the deep MOC cell reverses. The model's ACC total zonal volume transport and its components converge to near-constant values since the Southern Ocean essentially becomes decoupled from the northern hemisphere surface conditions.

[15] The other sequence of experiments with a constant vertical mixing gives very similar results. The key differences are that the model's ACC zonal volume transport is (10–15)% stronger and the strength of the abyssal MOC cell is weaker because there is less vertical diffusion in the abyss (not shown). Mesoscale eddies play an important role in the ACC dynamics by transferring momentum downward and attempting to restratify the region (i.e., they strive to flatten steep isopycnals). Thus we have also explored the sensitivity of our results to variations in diffusivity of applied eddy parameterization scheme. The outcome (after 1000 years) of the equivalent northern hemisphere warming experiments, with zero and a large (1000 m^2s^{-1}) uniform eddy diffusivity, show a consistent dependence of the ACC transport on the northern hemisphere surface buoyancy conditions, although details of the MOC and stratification, and the absolute values of the ACC transport differ quantitatively. The thermocline shoals and the ACC transport weakens with the increase of the eddy diffusivity because the slope of isopycnals is reduced.

4. Conclusions

[16] We have demonstrated that specified surface buoyancy increase in the Northern Hemisphere can produce a

striking intensification of the circumpolar current in the Southern Hemisphere in an equilibrium state of an idealized OGCM. This interhemispheric interaction stems from a steady-state requirement of the water mass conversion balance in conjunction with the cross-equatorial structure of the MOC and the thermocline. The applied reduction of the magnitude of the northern hemisphere SST meridional gradient affects the stratification at the northern edge of the Drake Passage and the buoyancy of the meridional return flow in the southern hemisphere circumpolar region; this changes the local meridional density gradient and consequently, though the thermal wind relation, the zonal volume transport of the model's ACC.

[17] The results are qualitatively, and to some degree quantitatively, insensitive to variations in the vertical mixing and mesoscale eddy parameterization schemes. In particular, the functional link between the increase of the northern hemisphere surface buoyancy and the increase of the southern hemisphere circumpolar volume transport is very robust to variations in these subgridscale closures. This interhemispheric link also shows robustness to variations in the Southern Ocean winds; a subset of experiments with a constant vertical mixing and southern hemisphere westerlies twice the amplitude of their northern hemisphere counterparts, conditions closer to those observed, displays the same effect (crosses in Figure 3).

[18] The importance of this result for the dynamics of the combined MOC-ACC system will of course depend on how robust it is in a high-resolution configuration with realistic bathymetry. The coarse resolution of our model combined with a limited zonal extent, flat boundaries, oversimplified Drake Passage geometry and the applied weak Southern Ocean wind constrains the MOC and the ACC values to be rather low, and the effects of having multiple ocean basins are missing. The use of an eddy parameterization cannot properly capture the role of mesoscale eddies in the ACC; the effect of transient eddies on the watermass transformation in the Southern Ocean mixed layer and feedbacks between stratification and eddy vertical momentum transfer are absent [*Henning and Vallis*, 2005; *Hallberg and Gnanadesikan*, 2006].

[19] **Acknowledgments.** We are grateful to Anand Gnanadesikan for useful discussions, and George Philander, Isaac Held and two anonymous reviewers for their comments and suggestions. The work was partially funded by the NSF.

References

Bryan, K., and L. J. Lewis (1979), A water mass model of the world ocean, *J. Geophys. Res.*, *84*, 2503–2517.

Conkright, M. E., et al. (2002), *World Ocean Database 2001*, vol. 1, *Introduction* [CD-ROM], NOAA *Atlas NESDIS*, vol. 42, edited by S. Levitus, 159 pp., U. S. Gov. Print. Off., Washington, D. C.

Gnanadesikan, A. (1999), A simple model for the structure of the oceanic pycnocline, *Science*, *283*, 2077–2079.

Gnanadesikan, A., and R. W. Hallberg (2000), On the relationship of the Circumpolar Current to Southern Hemisphere winds in coarse-resolution ocean models, *J. Phys. Oceanogr.*, *30*, 2013–2034.

Griffies, S. M., M. J. Harrison, R. C. Pacanowski, and A. Rosati (2004), A technical guide to MOM4, *GFDL Ocean Group Tech. Rep.*, *5*, 337 pp., NOAA Geophys. Fluid Dyn. Lab., Princeton, N. J.

Griffies, S. M., et al. (2005), Formulation of an ocean model for global climate simulations, *Ocean Sci.*, *1*, 45–79.

Hallberg, R., and A. Gnanadesikan (2006), The role of eddies in determining the structure and response of the wind-driven Southern Hemisphere overturning: Results from the Modeling Eddies in the Southern Ocean (MESO) project, *J. Phys. Oceanogr.*, *36*, 2232–2252.

Henning, C. C., and G. K. Vallis (2005), The effects of mesoscale eddies on the stratification and transport of an ocean with a circumpolar channel, *J. Phys. Oceanogr.*, *35*, 880–896.

Kalnay, E., et al. (1996), The NCEP/NCAR 40-year reanalysis project, *Bull. Am. Meteorol. Soc.*, *77*, 437–471.

Ledwell, J. R., A. J. Watson, and C. S. Law (1998), Mixing of a tracer in the pycnocline, *J. Geophys. Res.*, *103*, 499–529.

Rahmstorf, S. (1993), A fast and complete convection scheme for ocean models, *Ocean Modell.*, *101*, 9–11.

Samelson, R. M. (1999), Geostrophic circulation in a rectangular basin with a circumpolar connection, *J. Phys. Oceanogr.*, *29*, 3175–3184.

Samelson, R. M. (2004), Simple mechanistic models of middepth meridional overturning, *J. Phys. Oceanogr.*, *34*, 2096–2103.

Toggweiler, J. R., and B. L. Samuels (1995), Effect of the Drake Passage on the global thermohaline circulation, *Deep Sea Res., Part I*, *42*, 477–500.

Toggweiler, J. R., and B. L. Samuels (1998), On the ocean's large-scale circulation near the limit of no vertical mixing, *J. Phys. Oceanogr.*, *28*, 1832–1852.

Vallis, G. K. (2000), Large-scale circulation and production of stratification: Effect of wind, geometry and diffusion, *J. Phys. Oceanogr.*, *30*, 933–954.

Vallis, G. K. (2006), *Atmospheric and Oceanic Fluid Dynamics: Fundamentals and Large-Scale Circulation*, 745 pp., Cambridge Univ. Press, New York.

N. S. Fučkar and G. K. Vallis, Atmospheric and Oceanic Sciences Program, Princeton University, Forrestal Campus, Sayre Hall, Princeton, NJ 08544, USA. (nevensf@princeton.edu; gkv@princeton.edu)